

## Electrostatic interactions in tetrathiafulvalenium-tetracyanoquinodimethanide (TTF-TCNQ): Madelung energy and near-neighbor interactions

A. J. Epstein, N. O. Lipari, D. J. Sandman, and Paul Nielsen

Xerox Webster Research Center, Webster, New York 14580

(Received 23 June 1975)

The Madelung energy of tetrathiafulvalenium-tetracyanoquinodimethanide (TTF-TCNQ) has been calculated as a function of assumed charge transfer, charge distribution, and temperature, using a modified Evjen summing criterion. A large, temperature-independent, Madelung energy,  $E_M \approx -2.3$  eV/molecule ( $\approx -53$  kcal/mole), was calculated for the case of delocalized unit charges on the molecules.  $E_M$  alone is shown to be insufficient to stabilize charge transfer in TTF-TCNQ, and the polarization energy is shown to be the most plausible source of additional energy gain upon charge transfer. The near-neighbor Coulomb interactions are evaluated and shown to be the major source of energy gain upon charge delocalization on the molecule.

### I. INTRODUCTION

Organic donor-acceptor solids have been the subject of extensive recent study. These solids divide sharply into two classes<sup>1,2</sup>: (a) charge-transfer complexes and (b) charge-transfer salts. In the former class the crystalline solids formed are composed of closed-shell molecules which are essentially neutral in the ground state. In these systems, the lowest-energy electronic excitation is a charge transfer from the highest doubly occupied molecular orbital of the donor to the lowest empty molecular orbital of the acceptor. In the latter case the crystalline solids are composed of molecules which are essentially ionic. It is the open-shell nature of the molecular ions formed, together with their coalescing into segregated uniform stacks, which have led to the achievement of a metallic state in organic solids.<sup>3</sup> Compounds with the organic acceptor tetracyanoquinodimethane (TCNQ) may form either as charge-transfer complexes or charge-transfer salts depending upon the individual donor with which it is paired. For example, both anthracene-TCNQ (1:1) (Ref. 4) and carbazole-TCNQ (1:1) (Ref. 5) crystallize as charge-transfer complexes while the one-to-one alkali-metal-TCNQ compounds crystallize<sup>6</sup> as charge-transfer salts. Crystal structures for the two extreme classes are often quite similar, with parallel chains formed by the stacking of flat planar molecules. In the case of the charge-transfer complexes, stacks of alternate donor and acceptor are most common whereas the charge-transfer salts form both parallel segregated stacks of cations and anions and stacks with alternate cations and anions [e. g.,<sup>7</sup> tetramethyl-*p*-phenylenediamine-TCNQ (TMPD-TCNQ)] as well as noncolumnar structures.

Numerous TCNQ compounds have been reported to have multiple crystal phases and/or multiple observed stoichiometries. For example, crystals of the charge-transfer complex carbazole-TCNQ

are composed<sup>4</sup> of ordered and disordered domains. A number of the TCNQ salts including N-methylphenazinium-TCNQ,<sup>8,9</sup> and Rb-TCNQ,<sup>10</sup> have been reported to have several different stable crystal structures. Melby *et al.*<sup>11</sup> have reported that numerous donors form multiple stoichiometries with TCNQ including Cs (1:1 and 2:3), Cu (1:1 and 1:2) and N-methylphenazinium (1:1 and 1:2). This plenitude of crystal phases and stoichiometries is evidence for a subtle energetic balance upon formation of the solid phases of TCNQ compounds. Significant contribution to crystal binding is expected from a number of forces including electrostatic, van der Waals, and polarization. A detailed knowledge of the relative importance of these contributions is therefore important in understanding charge-transfer-salt formation in the various phases and stoichiometries.

We present here the results of an extensive numerical study of the electrostatic interactions of a TCNQ compound of current interest,<sup>12</sup> tetrathiafulvalenium-TCNQ (TTF-TCNQ). We have examined in detail the Madelung energy ( $E_M$ ) and its dependence upon assumed charge transfer, charge distribution, and temperature. In addition we have investigated the near-neighbor electrostatic interactions and their dependence upon charge distribution. We have found that though the electrostatic energy for the full charge-transferred configuration is significant ( $E_M \approx -2.3$  eV/molecule  $\approx -53$  kcal/mole) it alone is insufficient to account for the formation of a charge-transferred solid. Therefore other contributions to the crystalline energy were examined and a large degree of charge transfer was found to be energetically plausible.

Section II discusses the algorithm used to obtain the electrostatic energies. Section III presents the charge distributions and crystal structures we have used in our calculations. Section IV presents our numerical results for the Madelung energy and near-neighbor electrostatic interactions. Section V is a discussion of our results in light of available

physical data and estimates of other contributions to the crystal binding energy.

## II. COMPUTATIONAL APPROACH

The calculation of the electrostatic Madelung energy for real crystal systems is complicated by the slow inverse-length dependence of the Coulomb potential. Historically, two different approaches<sup>13,14</sup> have been utilized: (i) direct summation<sup>15,16</sup> using charge rearrangement to obtain rapid convergence, and (ii) use of mathematical transformations.<sup>17</sup> We have used a direct summation approach in performing our calculations in order to allow the study of the rapidity of convergence to the bulk electrostatic potentials and to enable the study of the direct electrostatic interactions of selected molecular pairs.

The Coulomb potential  $V_i$  at site  $i$  due to the presence of point charges  $q_j$  at sites  $j$  in the crystal is given by

$$V_i = \sum_{j \neq i} \frac{q_j}{|\vec{r}_j - \vec{r}_i|}, \quad (1)$$

where  $\vec{r}_i$  is the vector location of the  $i$ th site and the sum is extended over all sites in the infinite crystal except site  $i$ . Because the infinite series in Eq. (1) is only conditionally convergent,<sup>18</sup> the arrangement of the terms in the sum is of critical importance in obtaining the correct value.

Evjen<sup>16</sup> proposed the arrangement of the individual ions into elementary (neutral) cells, subsequent arrangement of the cells into shells about the center cell, and summation of the potentials of the individual shells rather than those of the individual ions. Evjen<sup>16</sup> and later authors<sup>13,19-21</sup> noted that neutrality of the elementary cell chosen was insufficient to guarantee convergence to (correct) unique values of the Coulomb potential at specific sites. Although the Coulomb potential of the elementary cell has a zero monopole term, dipole, quadrupole, and higher-order multipole contributions are possible. Because the Coulomb potential due to a dipole falls off slowly with distance ( $\sim r^{-2}$ ) and the dipole contribution of a shell increases with shell size ( $\sim r^2$ ), erroneous results may arise from use of elementary cells with a nonzero dipole moment. It can be shown<sup>13</sup> that if the elementary cell has zero dipole moment and finite quadrupole moment, then the Coulomb potentials found for the central elementary cell differ from the intrinsic Coulomb potentials by at most an additive constant, labeled here  $V_Q$ .

A modified Evjen summing algorithm was used in order to obtain the Madelung energy for TTF-TCNQ. Fractional charges were assigned to the atoms of each TTF and TCNQ molecule (see Sec. III). Because the individual atoms are not at symmetry points in the unit cell, the elementary cells

chosen to be used in the summation always have a finite quadrupole moment. In order to increase the rapidity of the convergence of the potential sum, elementary cells were added symmetrically about the center cell and the sum performed out to a specified radius (in units of the shortest crystallographic unit-cell axis). This modification is useful when the three unit-cell axes are quite unequal (e.g., 12.298, 3.819, and 18.468 Å for<sup>22</sup> TTF-TCNQ).

Since the elementary cells chosen have finite quadrupole moments, the Coulomb potentials found by using Eq. (1) include the additive quadrupole term  $V_Q$ . Thus the intrinsic Coulomb potential at site  $i$ ,  $V_i^i$ , is

$$V_i^i = V_i - V_Q. \quad (2)$$

This correction proves, however, to be of no great problem as the physically important parameters may be obtained in a manner in which  $V_Q$  cancels. For example, the difference in Coulomb potentials at two inequivalent sites  $j$  and  $k$  in the crystal  $\Delta_{jk}$ , which may be observable via core level x-ray photoemission splittings<sup>23</sup> is independent of  $V_Q$

$$\Delta_{jk} \equiv V_j^i - V_k^i = V_j - V_k. \quad (3)$$

Similarly, the Madelung energy  $E_M$  given by

$$E_M = \frac{1}{2} \sum_j q_j V_j^i - E_{\text{TTF}} - E_{\text{TCNQ}} \quad (4)$$

is independent of  $V_Q$  because the sum in the first term on the right-hand side of the equation is extended over a neutral pair of molecules (TTF<sup>+</sup> and TCNQ<sup>-</sup> or TTF<sup>0</sup> and TCNQ<sup>0</sup>) and

$$\frac{1}{2} \sum_j q_j V_j^i = \frac{1}{2} \sum_j q_j V_j - \frac{1}{2} V_Q \sum_j q_j = \frac{1}{2} \sum_j q_j V_j. \quad (5)$$

(The factor  $\frac{1}{2}$  is present in order to avoid double counting.) The other two terms on the right-hand side of Eq. (4) are the Coulomb self energies of the isolated TTF and TCNQ molecules. In order to verify the independence of our results from quadrupole effects, the calculations were performed assuming several different elementary cells of different quadrupole moment. The values for  $V_i$  obtained varied with the cell definition by as much as several volts but the values for  $\Delta_{jk}$ 's and  $E_M$  were always independent of cell choice.

The computer program utilized (EVJEN) was written and executed on Xerox Sigma 7 and Sigma 9 computers. Input parameters included the crystallographic unit-cell parameters (cell lengths and angles) for the system under study, the spatial coordinates and electrical charges of the unique atoms in the unit cell, and the maximum radius for the calculation. Subroutine CELL was used to build the neutral elementary cell used in the Evjen summing criterion. Several such subroutines were

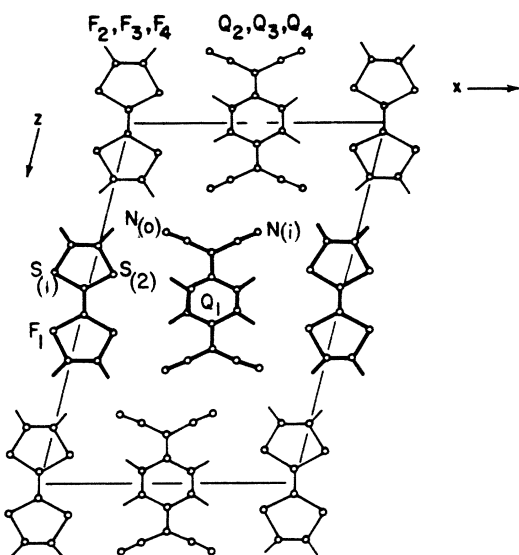


FIG. 1. View of the  $ac$  plane of the crystal packing in TTF-TCNQ (Ref. 22) (looking down the conducting or  $b$  axis). Shaded molecules have their centroids at  $v = \frac{1}{2}$ . Inequivalent nitrogen atoms,  $N_{(i)}$ , and  $N_{(o)}$ , are labeled as well as the inequivalent sulfur atoms,  $S_{(1)}$  and  $S_{(2)}$ .  $F_i$  and  $Q_i$  identify specific TTF and TCNQ molecules, respectively.

created to verify our results. Subroutine TRANSLATE was then used to build cells surrounding the center cell. DIPOLE and QUADRUPOLE subroutines calculated the respective moments of the elementary cell. The convergence of the Coulomb potentials calculated using EVJEN was rapid for TTF<sup>+</sup>-TCNQ<sup>-</sup>, being precise to two significant figures for a maximum radius of  $\sim 30$  Å, and precise to four significant figures for a maximum summing radius of  $\sim 75$  Å. The accuracy of our technique was verified through a calculation of the Madelung constant for the NaCl crystal structure. Agreement to seven significant

TABLE I. Crystal data for TTF-TCNQ.

	300 K <sup>a</sup>	100 K <sup>b</sup>	40 K <sup>b</sup>
$a$ (Å)	12.298	12.228	12.210
$b$ (Å)	3.819	3.754	3.729
$c$ (Å)	18.468	18.379	18.343
$\beta$	104.46°	104.42°	104.38°

<sup>a</sup>Reference 22.

<sup>b</sup>Reference 24.

figures with the accepted value was obtained.

### III. INPUT PARAMETERS

The TTF-TCNQ crystal structure has been extensively studied.<sup>22,24</sup> Figure 1 shows the room-temperature crystal structure<sup>22</sup> as seen looking down the conducting or  $b$  axis. Figure 2 is a side view<sup>22</sup> of the unit cell looking down the  $a$  axis showing the "herringbone" pattern characteristic of both adjacent TCNQ and adjacent TTF stacks. Individual TTF and TCNQ molecules are labeled  $F_i$  and  $Q_i$  for use in identifying near-neighbor interactions. Also labeled in Fig. 1 are the two nitrogen sites of TCNQ that are crystallographically inequivalent,  $N_{(i)}$  which nests inside an adjacent dicyanomethylene group, and  $N_{(o)}$  which is outside the  $bc$  plane of TCNQ molecules. Similarly the two crystallographically inequivalent sulfur atoms are labeled  $S_{(1)}$  and  $S_{(2)}$ . The bond lengths of both the TTF and TCNQ molecules indicate significant charge transfer.<sup>22,23</sup> The full crystal structure at 100 K has been reported<sup>24</sup> and was used for the 100-K Madelung energy calculations. The 100-K crystal structure was then used with the 40-K lattice constants to obtain the Madelung energy at 40 K. Table I summarizes the crystallographic data used.

The detailed molecular structure of TCNQ and TTF are shown in Figs. 3 and 4, respectively, along with the labeling of the unique atoms. Frac-

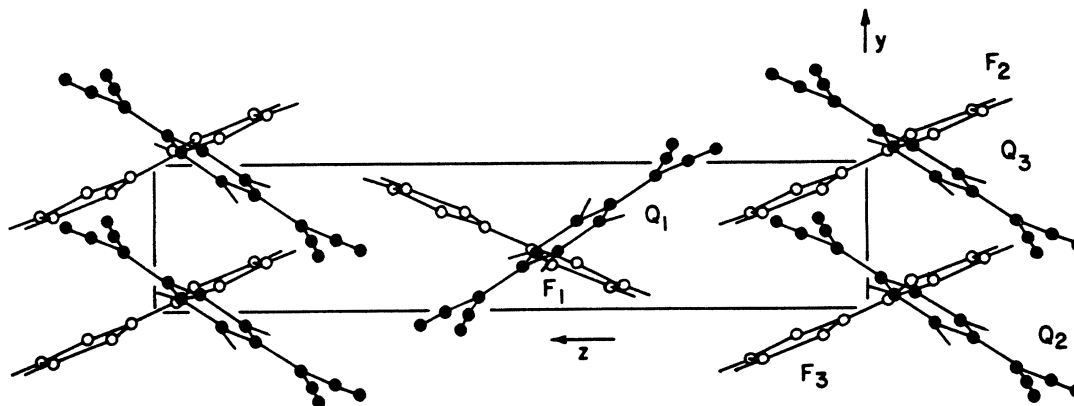


FIG. 2. View of the crystal packing in TTF-TCNQ looking down the  $a$  axis (Ref. 22). Shaded molecules have their centroids at  $x = \frac{1}{2}$ .  $F_i$  and  $Q_i$  identify specific TTF and TCNQ molecules, respectively.

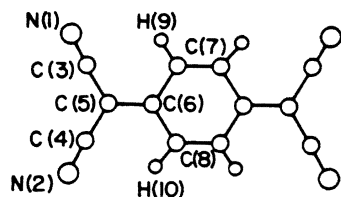


FIG. 3. Tetracyanoquinodimethane (TCNQ) molecule. The unique atoms for the TTF-TCNQ crystal structure are labeled.

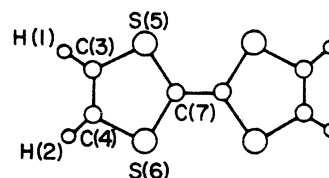


FIG. 4. Tetrathiafulvalene (TTF) molecule. The unique atoms for the TTF-TCNQ crystal structure are labeled.

tional point charges are assigned to each atom of each molecule. For simplicity in assigning charge distributions we have assumed that both the TTF and the TCNQ molecules have *mmm* symmetry, reducing the number of unique atoms on the TCNQ from ten to six [N(1), C(3), C(5), C(6), C(8), and H(9)] and on the TTF from seven to four [H(1), C(3), S(5), and C(7)]. This assumption has little effect upon the accuracy of our calculation. As is shown below, much larger variations in charge distribution lead to small variations in the Madelung energy.

The symmetrized charge distributions used for TCNQ<sup>0</sup>, TCNQ<sup>-</sup>, and TCNQ<sup>2-</sup> are given in Table II. The results obtained utilizing complete neglect of differential overlap methods (CNDO) are considered to be the most reliable (sets 1, 2, 6, 7, 15), with the charge distributions obtained using the CNDO/2 version<sup>25</sup> preferred over the CNDO-SCF version<sup>26,27</sup> results. They both predict an increase of charge of  $-0.14|e|$  at each nitrogen site upon going from TCNQ<sup>0</sup> to TCNQ<sup>-</sup>. This agrees very well with the results of nuclear-quadrupole-resonance experiments.<sup>25</sup> The PPP (Pople-Pariser-Parr<sup>28,36,37</sup>) and other results are included to test the sensitivity of the Madelung energy to the assumed charge distribution chosen. While differing in detail, all of the reasonable charge distributions place most of the

excess charge on the dicyanomethylene groups. This is illustrated for our CNDO/2 and CNDO-SCF results in Fig. 5, where it is seen that even TCNQ<sup>0</sup> has a large charge density on the individual atoms of the dicyanomethylene groups. However, it is shown later that this does not lead to any significant electrostatic contribution to the binding of a TTF-TCNQ crystal assumed composed of TTF<sup>0</sup> and TCNQ<sup>0</sup> molecules. Set 8 assigns  $\frac{1}{4}$  of the excess charge to each nitrogen in order to test the effects of partial charge delocalization. Set 12 represents a spin distribution for TCNQ<sup>-</sup> and as such places the excess "charge" closer to the center of the molecule. Set 9 places the excess charge at the center of the TCNQ<sup>-</sup> molecule itself.

Table III summarizes the symmetrized charge distributions for TTF<sup>0</sup>, TTF<sup>+</sup>, and TTF<sup>2+</sup>. Our CNDO/2 and CNDO-SCF results (sets 1, 2, 4, 5, and 9) are considered to be reliable for charge distributions with our CNDO/2 results preferred.<sup>27</sup> The calculations<sup>27</sup> were performed without inclusion of the sulfur *3d* levels. As illustrated in Fig. 5, the neutral TTF<sup>0</sup> molecule has very little net charge per atomic site (in contrast with TCNQ<sup>0</sup>) and TTF<sup>+</sup> has a relatively uniform charge distribution (again in contrast with TCNQ<sup>-</sup>). Set 6, which assigns  $\frac{1}{4}$  of each  $+|e|$  charge to each sulfur of TTF<sup>+</sup>, is an elementary charge distribution used to test the effects of moderate charge delocaliza-

TABLE II. Symmetrized charge distributions for tetracyanoquinodimethane. (Units of  $|e|$ .)

	Set	N(1)	C(3)	C(5)	C(6)	C(8)	H(9)	Ref.	Comment
TCNQ <sup>0</sup>	1	-0.161925	0.102575	0.0259	0.0628	-0.012725	0.027725	27	CNDO/2
	2	-0.286925	0.198775	-0.01084	0.08016	-0.09407	0.14756	27	CNDO-SCF
	3	-0.08613	0.07595	-0.00413	0.01503	0.00473	0.0	28	PPP
	4	-0.17911	0.14926	-0.01225	0.04349	0.01423	0.0	29	PPP
	5	-0.262	0.088	0.188	-0.212	-0.102	0.288	30	<i>Ab initio</i>
TCNQ <sup>-</sup>	6	-0.300675	0.128575	-0.10425	0.05595	-0.041225	-0.012525	27	CNDO/2
	7	-0.4284	0.2224	-0.1583	0.0937	-0.1276	0.1159	27	CNDO-SCF
	8	-0.25	0.0	0.0	0.0	0.0	0.0	...	Elementary distribution
	9	...	...	...	...	...	...	...	-1.0 at center of each TCNQ <sup>-</sup>
	10	-0.21359	0.12617	-0.24335	0.01705	-0.04943	0.0	31	PPP
	11	-0.27535	0.15973	-0.19916	0.0085	-0.03905	0.0	32	PPP
	12	-0.037	-0.007	-0.206	-0.072	-0.067	0.0	33	PPP (spin)
	13	-0.4945	0.2595	-0.0916	0.0512	0.0052	0.0	34	Hückel
	14	-0.379	0.091	0.051	-0.199	-0.129	0.241	30	<i>Ab initio</i>
	TCNQ <sup>2-</sup>	15	-0.38872	0.11452	-0.26995	0.05015	-0.0937	-0.0222	27

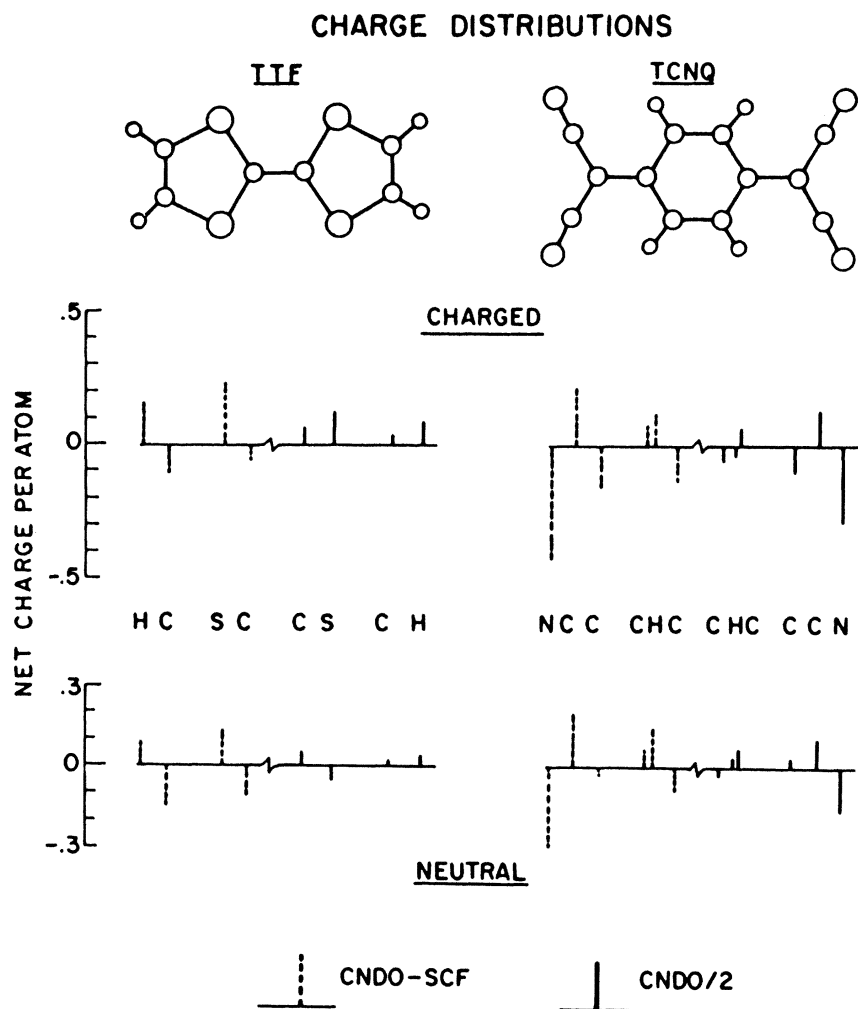


FIG. 5. CNDO/2 and CNDO-SCF charge distributions (Ref. 27) for TTF<sup>+</sup>, TTF<sup>0</sup>, TCNQ<sup>-</sup>, and TCNQ<sup>0</sup>. Net charge per atom is shown as a vertical bar for atoms labeled at the center of the figure (corresponding to the molecules drawn at the top of the figure). Charges on the left-hand side of each symmetric molecule illustrate our CNDO-SCF results, the right-hand side our CNDO/2 results. Note that the CNDO-SCF results have much larger variations in charge from atom to atom on a molecule, although both the CNDO-SCF and CNDO/2 charge distributions have similar overall spatial variation.

tion. Set 7 places the excess charge at the center of each TTF<sup>+</sup> molecule itself.

#### IV. NUMERICAL RESULTS

##### A. Madelung energy

Table IV enumerates our results for the Madelung energy at room temperature assuming one

full electron charge transferred from each TTF to each TCNQ.<sup>39</sup> The units are eV per TTF<sup>+</sup>-TCNQ<sup>-</sup> molecular pair. The differences in Coulomb potential (in volts) between the two inequivalent nitrogen sites  $\Delta N \equiv (V_{N(o)} - V_{N(i)})$ , and the two inequivalent sulfur sites  $\Delta S \equiv (V_{S(2)} - V_{S(1)})$  is also given in Table IV as calculated for each set of charge distributions. Runs 1-5 represent our main results. Runs 1 and

TABLE III. Symmetrized charge distributions for tetrathiafulvalene. (Units of  $|e|$ .)

	Set	H(1)	C(2)	S(5)	C(7)	Ref.	Comment
TTF <sup>0</sup>	1	0.0258	0.0060	-0.0550	0.0464	27	CNDO/2
	2	0.08824	-0.15229	0.1210	-0.1139	27	CNDO-SCF
	3	0.0085	-0.024	0.018	-0.005	28	CNDO/2
TTF <sup>+</sup>	4	0.0184	0.0245	0.1214	0.0454	27	CNDO/2
	5	0.1530	-0.1019	0.2263	-0.0548	27	CNDO-SCF
	6	0.0	0.0	0.25	0.0	...	Elementary distribution
	7	...	...	...	...	...	+1.0 at center of each TTF <sup>+</sup>
	8	0.063	-0.006	0.185	0.016	38	CNDO/2
TTF <sup>**</sup>	9	0.1361	0.0398	0.2927	0.0628	27	CNDO/2

TABLE IV. Madelung energies and Coulomb potential differences for  $\text{TTF}^+ - \text{TCNQ}^-$  at room temperature as a function of assumed charge distribution.

Run	TTF <sup>+</sup> Set	TCNQ <sup>-</sup> Set	$E_M$ (eV)	$\Delta N$ (V)	$\Delta S$ (V)
1	4	6	-2.27	1.51	0.47
2	5	7	-2.48	1.38	0.52
3	6	8	-1.97	1.30	0.40
4	4	12	-1.37	2.05	0.45
5	7	9	-0.57	...	...
6	4	10	-1.95	1.71	0.46
7	5	10	-2.22	1.65	0.46
8	4	11	-2.13	1.57	0.46
9	5	11	-2.39	1.51	0.46
10	4	13	-2.55	1.17	0.50
11	5	13	-2.77	1.10	0.50
12	4	14	-1.71	1.79	0.60
13	5	14	-1.94	1.73	0.60
14	8	6	-2.32	1.32	0.42
15	4	8	-2.04	1.78	0.52
16	5	8	-2.29	1.72	0.52
17	6	6	-2.23	1.03	0.34
18	6	7	-2.03	0.96	0.39
19	8	12	-1.53	1.86	0.40

2 are the most reliable results using our full delocalized charge distributions obtained through a CNDO/2 and CNDO-SCF routine, respectively. Run 3 assigns fractional charges to the nitrogens and sulfurs only. Run 4 uses a  $\text{TCNQ}^-$  spin distribution to represent the charge distribution in order to reduce the charge delocalization on  $\text{TCNQ}^-$ . Finally, Run 5 assumes  $+|e|$  at the center of each  $\text{TTF}^+$  and  $-|e|$  at the center of each  $\text{TCNQ}^-$ . Examining these five results it is clear that a reduction in charge delocalization reduces the attractive electrostatic Madelung energy while the effects upon  $\Delta N$  and  $\Delta S$  are not straightforward.

Runs 6–14 in Table IV summarize our results obtained using the various delocalized charge distributions available for  $\text{TTF}^+$  and  $\text{TCNQ}^-$ . Runs 15–19 assign either  $-0.25|e|$  per nitrogen or  $0.25|e|$  per sulfur. Comparing Runs 6–18 with 1 and 2 shows that the Madelung energy is relatively insensitive to variations in charge distribution pro-

TABLE V. Madelung energies and Coulomb potential differences for  $\text{TTF}^0 - \text{TCNQ}^0$  at room temperature as a function of assumed charge distribution.

Run	TTF <sup>0</sup> Set	TCNQ <sup>0</sup> Set	$E_M$ (eV)	$\Delta N$ (V)	$\Delta S$ (V)
1	1	1	0.00	-0.15	0.06
2	2	2	0.12	-0.47	0.07
3	1	3	-0.01	-0.06	0.04
4	2	3	-0.05	-0.28	0.00
5	1	4	0.01	-0.25	0.04
6	2	4	0.11	-0.47	0.00
7	1	5	-0.13	0.08	0.19
8	2	5	0.08	-0.14	0.15
9	3	1	0.07	-0.34	0.01

TABLE VI. Madelung energies and Coulomb potential differences as a function of temperature for  $\text{TTF} - \text{TCNQ}$ .

T (K)	$E_M$ (eV)	$\Delta N$ (V)	$\Delta S$ (V)
TTF <sup>+</sup> -TCNQ <sup>-</sup> (Delocalized: CNDO-SCF Charges)			
300 <sup>a</sup>	-2.48	1.38	0.52
100 <sup>b</sup>	-2.48	1.37	0.49
100 <sup>c</sup>	-2.49	1.40	0.53
40 <sup>d</sup>	-2.48	1.38	0.49
TTF <sup>+</sup> -TCNQ <sup>-</sup> (Localized: Point Charges)			
300 <sup>a</sup>	-0.57	...	...
100 <sup>b</sup>	-0.49	...	...
40 <sup>d</sup>	-0.45	...	...
TTF <sup>0</sup> -TCNQ <sup>0</sup> (Delocalized: CNDO-SCF Charges)			
300 <sup>a</sup>	0.12	-0.47	0.07
100 <sup>b</sup>	0.15	-0.52	0.03
40 <sup>d</sup>	0.15	-0.52	0.03

<sup>a</sup>300-K lattice constants and crystal structure (Ref. 22).

<sup>b</sup>100-K lattice constants and crystal structure (Ref. 24).

<sup>c</sup>100-K lattice constants (Ref. 24) and 300-K crystal structure (Ref. 22).

<sup>d</sup>40-K lattice constants (Ref. 24) and 100-K crystal structure (Ref. 24).

viding that most of the net charge on  $\text{TCNQ}^-$  remains on the dicyanomethylene groups. In contrast,  $\Delta N$  and  $\Delta S$  have considerably greater variation with assumed charge distribution. Run 19 assumes less charge delocalization on the  $\text{TCNQ}^-$  and agrees with the results shown for Run 4 in that  $E_M$  is significantly reduced. Summarizing the results in Table IV, for  $\text{TTF}^+ - \text{TCNQ}^-$  with complete charge transfer,  $E_M = -2.35 \pm 0.25$  eV,  $\Delta N = 1.45 \pm 0.3$  V, and  $\Delta S = 0.49 \pm 0.1$  V.

Table V presents the Madelung energy and Coulomb potential differences obtained using the full neutral charge distributions for  $\text{TTF}^0$  and  $\text{TCNQ}^0$  in the  $\text{TTF} - \text{TCNQ}$  crystal structure. Runs 1 and 2 use our charge distributions obtained via CNDO/2 and CNDO-SCF routines and are the most reliable results. It is clear that though there is a large spatial variation of charge on the  $\text{TCNQ}^0$  molecule itself,  $E_M \approx 0.0$  and  $\Delta N$  and  $\Delta S$  are similarly reduced close to zero. Comparing Tables IV and V, it is apparent that there is considerable energy gain upon charge transfer [ $\sim -2.3$  eV per ( $\text{TTF} + \text{TCNQ}$ )  $\sim -53$  cal/mole] as well as a large increase in difference between the Coulomb potential at the inequivalent nitrogen and sulfur sites.

The Madelung energy and Coulomb potential differences have been examined as a function of temperature for three specific charge distributions representing full charge transfer with charge delocalization (CNDO-SCF, Table II, Set 7 and Table III, Set 5), full charge transfer with no charge delocalization (point charge at the center of each

molecule, Table II, Set 9 and Table III, Set 7) and no charge transfer (CNDO-SCF, Table II, Set 2 and Table III, Set 2). The results (see Table VI) show that the Madelung energies calculated for the delocalized charge distributions are insensitive to the large contractions of the TTF-TCNQ unit cell (2.7% at 100 K and 3.7% at 40 K as compared with the room-temperature volume). In order to check if this insensitivity was due to the slight change in canting angle of the TTF molecule upon contraction from room temperature to 100 K, the calculation was redone assuming the 100-K lattice constants and the 300-K crystal structure. The results were found to be insensitive to this change. Hence electrostatic interactions neither drive nor hinder the lattice contraction and the slight molecular canting observed as the temperature is lowered.

#### B. Near-neighbor interactions

The flexibility of the EVJEN program allows the straightforward calculation of the electrostatic interaction between any specified pair of atoms or molecules. These calculations are exact, without the complication of a quadrupole potential, because they involve only finite sums. The mutual electrostatic energy (energy per pair of molecules) is given in Table VII for all near-neighbor pairs of molecules in the TTF<sup>+</sup>-TCNQ<sup>-</sup> crystal structure for two different reasonable delocalized charge distributions [CNDO/2 (Table II, Set 6 and Table III, Set 4) and CNDO-SCF (Table II, Set 7 and Table III, Set 5)] as well as for point charges at each molecular ion center (Table II, Set 9 and Table III, Set 7). The molecular labels  $F_i$  (for TTF molecules) and  $Q_i$  (for TCNQ molecules)

refer to specific molecules in Figs. 1 and 2. Comparison of the results for the CNDO/2 and CNDO-SCF charge distributions show only small differences in the near-neighbor electrostatic interactions found despite large differences in their detailed charge densities per atom. This is consistent with the nearly identical Madelung energies calculated using the two charge distributions (-2.27 and -2.48 eV, respectively). Comparison with the near-neighbor results found by assuming unit point charges at the center of each molecule shows charge delocalization leads to a large reduction in the nearest-neighbor Coulomb repulsion [TCNQ molecules  $Q_2$  and  $Q_3$  ( $Q_2Q_3$ ) and TTF molecules  $F_2$  and  $F_3$  ( $F_2F_3$ )] and a smaller reduction in the nearest-neighbor Coulomb attraction ( $F_1Q_1$ ).

The difference in Madelung energy between that of the delocalized charge distributions ( $\approx -2.35$  eV) and that of the localized charge distributions (-0.57 eV) is found to be approximately equal to the sum of the differences in their nearest-neighbor interactions listed in Table VII. That is,

$$Q_2Q_3 + Q_2Q_4 + 2Q_1Q_2 + F_2F_3 + F_2F_4 + 2F_1F_2 \\ + 2F_1Q_1 + 2F_2Q_1 + 2F_3Q_1 + 2F_1Q_2 + 2F_1Q_3 + 4F_2Q_2$$

is equal to -7.01 and -7.02 eV for CNDO/2 and CNDO-SCF charge distributions, respectively, and -5.66 eV for the point charges. (Note that for purposes of comparing to the Madelung energy, the number of each type of near-neighbor interactions appearing in this sum has been halved to avoid double counting.) Examining these numbers it is clear that (a) charge delocalization is most important in the near-neighbor interactions, and (b) the net interaction with the near-neighbor environment

TABLE VII. Mutual electrostatic energy (eV per pair of molecules) for near-neighbor pairs of molecules of TTF<sup>+</sup>-TCNQ<sup>-</sup>.

Molecular pair <sup>a</sup>	Charge distribution			Point	Comment
	CNDO/2	CNDO-SCF	Point		
$Q_2 Q_3$	2.37	2.24	3.77	Nearest-neighbors within stack.	
$Q_2 Q_4$ <sup>b</sup>	1.59	1.54	1.88	Second nearest-neighbors within stack.	
$Q_1 Q_2$	1.69	1.74	1.53	Nearest-neighbors between stacks.	
$Q_1 Q_3$	1.69	1.74	1.53	Same as $Q_1 - Q_2$ .	
$F_2 F_3$	2.85	2.73	3.77	Nearest-neighbors within stack.	
$F_2 F_4$ <sup>b</sup>	1.72	1.69	1.88	Second nearest-neighbors within stack.	
$F_1 F_2$	1.69	1.68	1.53	Nearest-neighbors between stacks.	
$F_1 F_3$	1.69	1.68	1.53	Same as $F_1 - F_3$ .	
$F_1 Q_1$	-2.00	-1.88	-2.34	Nearest-neighbor TTF, TCNQ.	
$F_2 Q_2$	-1.87	-1.87	-1.99	Same as $F_3 - Q_3$ . See Figs. 1 and 2.	
$F_2 Q_1$	-1.63	-1.65	-1.45	See Figs. 1 and 2.	
$F_3 Q_1$	-1.42	-1.40	-1.45	See Figs. 1 and 2.	
$F_1 Q_2$	-1.21	-1.22	-1.16	See Figs. 1 and 2.	
$F_1 Q_3$	-1.15	-1.14	-1.16	See Figs. 1 and 2.	

<sup>a</sup>See Figs. 1 and 2 for molecular positions.

<sup>b</sup>Not shown in Figs. 1 and 2.

is strongly attractive implying that the longer-range contribution is repulsive.

For ionic crystalline materials with integral charges per ion, the dimensionless Madelung constant  $\alpha$  is defined<sup>14</sup> as

$$\alpha \equiv -(ze^2/R)^{-1} E_M, \quad (6)$$

where  $E_M$  is the Madelung energy per "neutral molecule,"  $z$  is the largest common factor for the ionic charges, and  $R$  is the nearest-neighbor distance. The Madelung constant is independent of the absolute value of the ionic charges and of the absolute value of the unit-cell dimensions; it depends only upon the crystal structure and provides a measure of the relative effects of the total (including long-range) and nearest-neighbor contributions to the electrostatic binding energy. Following Metzger,<sup>40</sup> the equivalent Madelung constant is defined for the organic salts with delocalized (fractional) charges on each atom of the molecular ions as the ratio of crystalline Madelung energy  $E_M$  to the nearest-neighbor attractive interaction  $F_1Q_1$ . The results are

$$\alpha \equiv \frac{E_M}{F_1Q_1} = \begin{cases} 1.14, & \text{CNDO/2} \\ 1.32, & \text{CNDO-SCF} \\ 0.24, & \text{POINT} \end{cases} \quad (7)$$

Thus delocalization of charge on the molecules considerably increases the net non-nearest neighbor contribution to the electrostatic energy. Comparison with  $\alpha_{\text{NaCl}} = 1.75$  shows that although the TTF-TCNQ crystal structure does lead to a much smaller Madelung constant for unit point charges, charge delocalization does bring  $\alpha$  to a regime

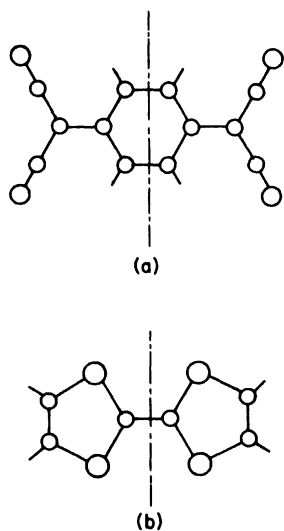


FIG. 6. (a) Assumed division of  $\text{TCNQ}^{2-}$  into two monocation halves. (b) Assumed division of  $\text{TTF}^{2+}$  into two monocation halves.

TABLE VIII. On-site ( $U_0$ ) and nearest-neighbor ( $U_1$ ) mutual Coulomb energies (eV) for  $\text{TTF}^+ - \text{TCNQ}^-$  using CNDO/2 charge distribution.

	TCNQ	TTF
$U_0$	2.33	3.17
$U_1$	2.37	2.85
$(U_0 - U_1)$	-0.04	0.32

where considerable electrostatic stabilization is possible.

During charge transport along a uniform stack of singly charged molecular ions, electrons (holes) will move and doubly occupy some sites resulting in the formation of dianions (dications) and adjacent neutral molecules. This changes some of the terms in the electrostatic interaction sum [Eq. (4)]. Examining a single such charge transfer along a  $\text{TCNQ}^-$  ( $\text{TTF}^+$ ) stack, the net result is the loss of one nearest-neighbor Coulomb repulsion within a stack,<sup>41</sup>  $U_1$  ( $Q_2Q_3$  or  $F_2F_3$ ), and the gain of an onsite Coulomb repulsion between the two excess charges of the resulting di-ion,  $U_0^{41}$ . (This assumes that all interaction energies between each electron of the di-ion and all singly charged molecules remain unchanged.) The difference in these energies  $U \equiv U_1 - U_0$  reduced by the presence of nearby polarizable molecules, is important for determining whether a specific organic salt is metallic or a magnetic insulator.<sup>41</sup> Therefore, using our CNDO/2 charge distributions for  $\text{TCNQ}^-$  and  $\text{TTF}^{2+}$  (Tables II and III) we have calculated the onsite Coulomb repulsions,  $U_{0Q}$  and  $U_{0F}$ . This was done assuming strong correlation of the charges on the di-ion in order to reduce their mutual Coulomb repulsion. Hence a Heitler-London approach was used with molecular charges divided into two halves as shown in Fig. 6. The net Coulomb repulsion between each half was then computed using EVJEN. This procedure probably underestimates  $U_0$  as delocalization of the charges from the fully correlated state assumed would lead to greater overlap and increase Coulomb repulsion.

Our CNDO/2 results are shown in Table VIII. Almost identical  $(U_0 - U_1)$  values were obtained using CNDO-SCF charge distributions. The most important point is that  $U_{0Q} \approx U_{1Q}$  and therefore  $U_{0Q} - U_{1Q} \approx 0$  while  $U_{0F} - U_{1F} \approx 0.3$  eV. In reality, because  $U_{0Q}$  and  $U_{0F}$  are underestimated  $U_0 - U_1$  is expected to be considerably larger for both the  $\text{TCNQ}^-$  stacks and  $\text{TTF}^+$  stacks.  $U_0$  and  $U_1$  would then be reduced through the presence of neighboring polarizable molecules. Examining these bare  $(U_0 - U_1)$  values, it is evident that for the given intrachain intermolecular geometry of  $\text{TTF}^+ - \text{TCNQ}^-$ , the  $\text{TCNQ}^-$  chain would more likely have  $U_0 - U_1 \approx 0$ . Thus charge-transfer salts of  $\text{TTF}^+$  with other

anions which exhibit this TTF<sup>+</sup> intrachain intermolecular geometry are more likely to show Coulomb effects than charge-transfer salts of TCNQ<sup>-</sup> which exhibit this TCNQ<sup>-</sup> intrachain intermolecular geometry.

### V. DISCUSSION

The Madelung energy per (TTF<sup>+</sup> - TCNQ<sup>-</sup>) of -2.35 eV in the full charge-transferred limit is the largest electrostatic energy found so far for an organic salt with segregated stacks of planar donors and planar acceptors. In contrast,  $E_M$  for the segregated stack salt (N-methylphenazinium)<sup>+</sup>TCNQ<sup>-</sup> was reported by Metzger<sup>42</sup> to be approximately zero, while organic salts with monoatomic cations or anions,<sup>40,43</sup> and alternate donor-acceptor stacks<sup>44</sup> show much larger Madelung energies. For all organic salts, however,  $E_M$  is much smaller than that of the simple inorganic salts<sup>14</sup> such as Na<sup>+</sup>Cl<sup>-</sup> ( $E_M = -11.05$  eV per molecule).

Of fundamental importance is whether or not  $E_M$  is sufficient to stabilize charge transfer in the given TTF-TCNQ crystal, and if not, what terms contribute to the stabilization in addition to  $E_M$ . For a given crystal structure, the crystal binding energy  $E_c$  is approximately given by

$$E_c^0 \cong E_{\text{vdW}}^0 + E_{\text{CR}}^0 \quad (8a)$$

for neutral molecules and

$$E_c^\rho \cong \rho(I - A) + \rho^2 E_M + \rho^2 E_{\text{ex}} + \rho^2 E_{\text{po1}} + E_B^\rho + E_{\text{vdW}}^\rho + E_{\text{CR}}^\rho \quad (8b)$$

for the charge-transferred case.

Here  $\rho$  is the fractional degree of charge transfer with the superscript zero indicating no charge transfer,  $E_{\text{vdW}}$  is the van der Waals energy,  $E_{\text{CR}}$  is the core repulsion energy,  $I$  is the gas-phase ionization energy of the neutral donor,  $A$  is the gas-phase electron affinity of the neutral acceptor,  $E_{\text{ex}}$  is the exchange energy which is included because the calculation for  $E_M$  assumed disjoint charges on each site and in reality there is electron wave-function overlap for molecules along the chain,  $E_{\text{po1}}$  is the polarization energy gained through interaction with dipoles induced on neighboring sites, and  $E_B^\rho$  is the energy gained through delocalization of the hole or excess electron into an energy band of finite width. Equation (8b) is a crude approximation used to show the general functional dependence of  $E_c$  with  $\rho$ . As formulated in Eq. (8b),  $E_c^\rho$  is a minimum at either  $\rho=0$  or 1 and at no value between (see below). For the charge-transferred configuration to be stable the free energy of the crystal  $F_c^\rho = E_c^\rho - TS$  must satisfy  $F_c^\rho < F_c^0$  for some range of  $\rho$ . Assuming that the degree of charge transfer is independent of temperature (as may be inferred from the temperature dependence of the crystallographic measure-

ments<sup>24</sup>), the condition for the formation of a stable charge-transferred configuration reduces to  $E_c^\rho < E_c^0$ .

In simple inorganic salts,  $E_M$  alone is sufficient to stabilize charge transfer ( $|E_M| > I - A$ ). For TTF, the gas-phase ionization energy is<sup>45</sup> 6.81 eV (6.83 eV)<sup>46</sup> while the gas-phase electron affinity of TCNQ is reported<sup>47</sup> to be 2.8 eV. The difference (4.0 eV) is 1.7 eV larger than  $|E_M|$ . Hence  $E_M$  alone is *insufficient* to stabilize charge-transfer in TTF-TCNQ. The remaining terms in Eq. (8b) are not explicitly known although rough estimates can be made. The exchange energy  $E_{\text{ex}}$  is expected to be much smaller than  $E_M$  and hence insufficient to stabilize TTF-TCNQ. (It was estimated<sup>48</sup> it to be  $\sim 0.5$  eV for the alternate donor-acceptor systems.) The exchange energy is zero for zero charge transfer [Eq. (8a)]. The energy owing to delocalization of electrons (holes) in the conduction band is of order one-quarter the bandwidth or<sup>12</sup>  $\approx 0.1$  eV (see below) and is insufficient to make  $E_c^\rho < E_c^0$ .

The last two terms in Eq. (8b) are similar to those in Eq. (8a). The core repulsion energy is probably independent of charge transfer. Van der Waals energies for neutral closed-shell molecular materials are of order 1.0 eV, as for example in anthracene.<sup>49</sup> It is unlikely that  $E_{\text{vdW}}^\rho$  differs greatly from  $E_{\text{vdW}}^0$  although it may change as in the charge-transferred configuration, we are then dealing with open-shell molecules.

The remaining term in Eq. (8b) ( $E_{\text{po1}}$ ) can, however, be sufficiently large and attractive to cause a charge-transferred configuration to be the more energetically favorable one. The energy required for ionization of neutral TTF<sup>0</sup> or neutral TCNQ<sup>0</sup> in a homomolecular solid  $I_c$  differs from the gas-phase ionization energy  $I_g$  by an amount  $P$  owing to the energy gained in polarizing the neutral lattice surrounding the remaining cation.<sup>50,51</sup> Subtracting the solid-state threshold ionization energies for TTF<sup>0</sup> and TCNQ<sup>0</sup> of<sup>52</sup> 5.0 and 7.88 eV, respectively, from their gas-phase ionization energies of 6.81,<sup>45</sup> and 9.61 eV,<sup>53</sup> respectively, it is seen that  $P \approx 1.8$ , or  $E_{\text{po1}} = -3.6$  eV per "TTF-TCNQ" molecule. A more conservative estimate of the polarization energy than that obtained by the conventional approach<sup>50</sup> just outlined may be made by subtracting the ionization energy for the center of the peak corresponding to the highest occupied molecular orbital in the solid phase, from that in the gas phase. Using our values for the solid-state ionization energy at the peak of 5.6 to 5.9 eV for TTF<sup>0</sup> and 8.53 eV for TCNQ<sup>0</sup>,  $P$  because -1.2 to -0.9 eV for TTF<sup>0</sup> and -1.1 eV for TCNQ<sup>0</sup>. Therefore,  $E_{\text{po1}} \approx -2.0$  eV per "TTF-TCNQ" molecule. This is in agreement with previous estimates of an increase in the cohesive en-

ergy per TCNQ molecule owing to polarization of the lattice of  $\sim 1$  eV obtained using a small polaron approach.<sup>54,55</sup>

Although the functional dependence upon  $\rho$  is uncertain, it is clear that  $E_{\text{po1}}$  may be sufficiently large to stabilize the charge-transferred configuration ( $E_c^p < E_c^0$ ). For the charge-transferred configuration, two effects may invalidate our estimate for  $E_{\text{po1}}$ : (a) Polarization of the lattice due to unlike charges on adjacent sites tends to cancel. This may be offset by increased attractive energy owing to addition of polarization because of like charges on adjacent sites in the chain. (b) The polarization energy associated with a lattice of open-shell molecules may be considerably different than that estimated from the lattice formed of neutral closed-shell molecules. Despite the uncertainties of our estimate, it is clear that  $E_{\text{po1}}$  can easily be the primary source of the additional 1.7 eV necessary to stabilize charge transfer in TTF-TCNQ.

The energetics of fractional charge transfer<sup>56</sup> in TTF-TCNQ<sup>57-60</sup> have been examined especially in terms of the  $\rho$  dependence of  $E_M$ . As we indicated above, the exact  $\rho$  dependence of  $E_{\text{po1}}$ ,  $E_{\text{vdw}}^p$ , and  $E_{\text{CR}}^p$  is uncertain. Examination of the remaining terms on the right-hand side of Eq. (8b) shows that though the  $\rho$  dependence of  $(I-A)$  is straightforward, the other energies require further review. Thus while  $E_M$  and  $E_{\text{ex}}$  are indicated in Eq. (8b) to vary as  $\rho^2$ , for the real material this is not exactly true as the (normalized) charge distribution on both TTF<sup>+ $\rho$</sup>  and TTF<sup>- $\rho$</sup>  will depend on  $\rho$  (e.g., the charge distributions of TTF<sup>0</sup> and TCNQ<sup>0</sup> are not uniformly zero on each atom).  $E_B$ , the energy per "TTF-TCNQ molecule" gained through delocalization of electrons in a band of width  $W_Q$  and holes into a band of width  $W_F$  can be exactly calculated as a function of  $\rho$  in a tight-binding band theory<sup>61</sup> limit

$$E_B = -(1/\pi)(W_F + W_Q) \sin^2 \frac{1}{2} \rho \pi. \quad (9)$$

Though significant,  $E_B$  is insufficient to stabilize charge transfer alone. Its trigonometric dependence on  $\rho$  may, however, help to stabilize a fractional charge-transfer state as functional dependencies of  $E_c^p$  on  $\rho$  other than linear or quadratic are necessary to achieve stabilization of fractional charge transfer.

Experimentally, x-ray bond lengths<sup>23</sup> and photoemission<sup>23,52,62-64</sup> indicate significant charge

transfer. In particular the observed<sup>62</sup> splitting of the N 1s core-level x-ray photoemission line of  $\sim 1.4$  eV had been assigned<sup>62</sup> to the presence of two types of TCNQ in TTF-TCNQ, TCNQ<sup>0</sup> and TCNQ<sup>-</sup>, implying incomplete charge transfer. We have previously shown,<sup>23</sup> using our CNDO-SCF charge distributions for TCNQ<sup>-</sup>, TCNQ<sup>0</sup>, TTF<sup>+</sup>, and TTF<sup>0</sup> that this splitting, as well as a splitting<sup>64</sup> of 0.8 eV of the x-ray photoemission S 2p line, could be accounted for by the difference in Coulomb potential at the inequivalent nitrogen sites and inequivalent sulfur sites in the crystal structure (see Fig. 1). Examining the values listed for  $\Delta N$  and  $\Delta S$  for different charge distributions, it is clear that these core level splittings can be accounted for by Coulomb potential differences although an accurate estimate of the degree of charge transfer cannot be made from the comparison with the experimental splittings because of the variations in  $\Delta N$  and  $\Delta S$  calculated. Detailed examination of the convergence of the Coulomb potential sums [Eq. (1)] in real space using EVJEN indicates that the surface layer of molecules which are probed by photoemission<sup>23,65</sup> have different Coulomb potentials than the bulk atoms.

The crystal-field-split core levels examined by x-ray photoemission spectroscopy therefore need not exhibit equal intensity. New ultraviolet photoemission experiments<sup>65</sup> on multilayer TTF-TCNQ of precisely defined compositions show greater than 40% charge transfer even at  $\sim 100$  K; and recent x-ray diffuse scattering data<sup>66</sup> suggest  $\approx 60\%$  charge transfer. These results are consistent with our analysis.

The near-neighbor electrostatic interactions found show that the energy gained through charge delocalization onto the molecules is greatest for near-neighbor interactions. This energy gain combined with a relatively low onsite Coulomb repulsion for TCNQ<sup>-</sup>,  $U_{0Q}$ , implies that the symmetry of TCNQ with its electron-withdrawing dicyanomethylene groups at either end of the quinoid ring may be very important in gaining the ability to form crystals with segregated stacks of TCNQ<sup>-</sup>.

*Note added in proof:* Two other groups have now reported similar numerical results for  $E_M$  of TTF<sup>+</sup>-TCNQ<sup>-</sup>:  $E_M = -(2 \pm 0.2)$  eV,<sup>67</sup> and  $-2.4 \lesssim E_M \lesssim -1.9$  eV.<sup>68</sup> The latter value was obtained using the Ewald technique<sup>17,40</sup> and both are in good agreement with our result of  $E_M = -(2.35 \pm 0.25)$  eV obtained by the Evjen approach.

<sup>1</sup>F. H. Herbstein, *Perspectives in Structural Chemistry*, edited by J. D. Dunitz and J. A. Ibers (Wiley, New York, 1971), Vol. IV, p. 166; R. P. Shibaeva and L. O. Atovmyan, *J. Struct. Chem.* **13**, 546 (1972).

<sup>2</sup>P. L. Nordio, Z. G. Soos, and H. M. McConnell, *Ann. Rev. Phys. Chem.* **17**, 237 (1966); Z. G. Soos, *ibid.* **25**, 121 (1974).

<sup>3</sup>A. F. Garito and A. J. Heeger, *Acc. Chem. Res.* **7**,

- 232 (1974).
- <sup>4</sup>R. M. Williams and S. C. Wallwork, *Acta Crystallogr. B* **24**, 168 (1968).
- <sup>5</sup>H. Kobayashi, *Bull. Chem. Soc. Jpn.* **46**, 2675 (1973).
- <sup>6</sup>A. Hoekstra, T. Spoelder, and A. Vos, *Acta Crystallogr. B* **28**, 14 (1972); I. Shirovani and H. Kobayashi, *Bull. Chem. Soc. Jpn.* **46**, 2595 (1973).
- <sup>7</sup>A. W. Hanson, *Acta Crystallogr.* **19**, 610 (1965).
- <sup>8</sup>C. J. Fritchie, Jr., *Acta Crystallogr.* **20**, 892 (1966).
- <sup>9</sup>L. B. Coleman, S. K. Khanna, A. F. Garito, A. J. Heeger, and B. Morosin, *Physics Lett. A* **42**, 15 (1972).
- <sup>10</sup>A. Hoekstra, T. Spoelder, and A. Vos, *Acta Crystallogr. B* **28**, 14 (1972); I. Shirovani and H. Kobayashi, *Bull. Chem. Soc. Jpn.* **46**, 2595 (1973).
- <sup>11</sup>L. R. Melby, R. J. Harder, W. R. Hertler, R. Mahler, R. E. Benson, and W. E. Mochel, *J. Am. Chem. Soc.* **84**, 3374 (1962); L. R. Melby, *Can. J. Chem.* **43**, 1448 (1965).
- <sup>12</sup>A. J. Heeger and A. F. Garito, in *Proceedings of the NATO Summer Institute on Low Dimensional Conductors*, edited by H. J. Keller (Plenum, New York, 1975), p. 89.
- <sup>13</sup>A. Redlack and J. Grindlay, *J. Phys. Chem. Solids* **36**, 73 (1975).
- <sup>14</sup>M. P. Tosi, in *Solid State Physics*, edited by F. Seitz and D. Turnbull (Academic, New York, 1964); Vol. 16, p. 1.
- <sup>15</sup>E. Madelung, *Z. Phys.* **19**, 524 (1918).
- <sup>16</sup>E. Evjen, *Phys. Rev.* **39**, 675 (1932).
- <sup>17</sup>P. P. Ewald, *Ann. Phys. (Leipz.)* **64**, 253 (1921).
- <sup>18</sup>E. L. Burrows and S. F. A. Kettle, *J. Chem. Educ.* **52**, 58 (1975).
- <sup>19</sup>K. S. Krishnan and S. K. Roy, *Phys. Rev.* **87**, 581 (1952).
- <sup>20</sup>I. D. C. Gurney, *Phys. Rev.* **90**, 317 (1953).
- <sup>21</sup>S. K. Roy, *Can. J. Phys.* **32**, 509 (1954).
- <sup>22</sup>T. J. Kistenmacher, T. E. Phillips, and D. O. Cowan, *Acta Crystallogr. B* **30**, 763 (1974).
- <sup>23</sup>A. J. Epstein, N. O. Lipari, P. Nielsen, and D. J. Sandman, *Phys. Rev. Lett.* **34**, 914 (1975); *Bull. Am. Phys. Soc.* **20**, 465 (1975).
- <sup>24</sup>R. H. Blessing and P. Coppens, *Solid State Commun.* **15**, 215 (1974).
- <sup>25</sup>J. A. Pople and G. A. Segal, *J. Chem. Phys.* **43**, 5129 (1965); *ibid.* **43**, 5136 (1965); *ibid.* **44**, 3289 (1966).
- <sup>26</sup>N. O. Lipari and C. B. Duke, *J. Chem. Phys.* **63**, 1748 (1975); C. B. Duke, N. O. Lipari, W. Salaneck, and L. B. Schein, *ibid.* **63**, 1758 (1975); N. O. Lipari and C. B. Duke, *ibid.* **63**, 1768 (1975).
- <sup>27</sup>N. O. Lipari, A. J. Epstein, P. Nielsen, J. J. Ritsko, and D. J. Sandman (unpublished).
- <sup>28</sup>D. A. Lowitz, *J. Chem. Phys.* **46**, 4698 (1967). Table VII, Set 1.
- <sup>29</sup>Reference 28, Table VII, Set 2.
- <sup>30</sup>H. T. Jonkman, G. A. van der Velde, and W. C. Nieuwpoort, *Chem. Phys. Lett.* **25**, 62 (1974).
- <sup>31</sup>Reference 28, Table VII, Set 3.
- <sup>32</sup>Reference 28, Table VII, Set 7.
- <sup>33</sup>Reference 28, Table VI, Set 3.
- <sup>34</sup>E. Menefee and Y.-H. Pao, *J. Chem. Phys.* **36**, 3472 (1972).
- <sup>35</sup>J. Murgich and S. Pissanetzky, *Chem. Phys. Lett.* **18**, 420 (1973).
- <sup>36</sup>J. A. Pople, *Trans. Faraday Soc.* **49**, 1375 (1953).
- <sup>37</sup>R. Pariser and R. G. Parr, *J. Chem. Phys.* **21**, 466 (1953); *ibid.* **21**, 767 (1953).
- <sup>38</sup>M. A. Ratner, J. R. Sabin, and E. E. Ball, *Chem. Phys. Lett.* **28**, 393 (1974).
- <sup>39</sup>These results were initially reported at the March 1975 American Physical Society Meeting, Denver, Colorado; A. J. Epstein, N. O. Lipari, D. J. Sandman, and P. Nielsen, *Bull. Am. Phys. Soc.* **20**, 465 (1975).
- <sup>40</sup>R. M. Metzger, *J. Chem. Phys.* **57**, 1870 (1972).
- <sup>41</sup>A. J. Epstein, S. Etemad, A. F. Garito, and A. J. Heeger, *Phys. Rev. B* **5**, 952 (1972).
- <sup>42</sup>R. M. Metzger, *J. Chem. Phys.* **57**, 2218 (1972).
- <sup>43</sup>M. Konno, H. Kobayashi, F. Marumo, and Y. Saito, *Bull. Chem. Soc. Jpn.* **46**, 1987 (1973).
- <sup>44</sup>R. M. Metzger, *J. Chem. Phys.* **57**, 1876 (1972).
- <sup>45</sup>D. J. Sandman, P. Nielsen, A. J. Epstein, N. O. Lipari, and G. P. Ceasar, 169th National Meeting, American Chemical Society, Philadelphia, Pennsylvania, April 6-11, 1975, Abstracts of Papers ORGN 46; and (unpublished).
- <sup>46</sup>R. Gleiter, E. Schmidt, D. O. Cowan, and J. P. Ferraris, *J. Electron Spectrosc. Relat. Phenom.* **2**, 207 (1973).
- <sup>47</sup>C. E. Klots, R. N. Compton, and V. F. Raaen, *J. Chem. Phys.* **60**, 1177 (1974).
- <sup>48</sup>Z. G. Soos and A. J. Silverstein, *Mol. Phys.* **23**, 775 (1972).
- <sup>49</sup>E. F. Westrum, Jr., and J. P. McCullough, in *Physics and Chemistry of the Organic Solid State*, edited by D. Fox, M. M. Labes, and A. Weissberger (Interscience, New York, 1963), Vol. 1, p. 1.
- <sup>50</sup>F. Gutman and L. E. Lyons, *Organic Semiconductors* (Wiley, New York, 1967), Chap. 6.
- <sup>51</sup>M. Batley, L. J. Johnston, and L. E. Lyons, *Aust. J. Chem.* **23**, 2397 (1970).
- <sup>52</sup>P. Nielsen, A. J. Epstein, and D. J. Sandman, *Solid State Commun.* **15**, 53 (1974).
- <sup>53</sup>I. Ikemoto, K. Samizo, T. Fujikawa, K. Ishii, T. Ohta, and H. Kuroda, *Chem. Lett.* **7**, 785 (1974).
- <sup>54</sup>P. M. Chaikin, A. F. Garito, and A. J. Heeger, *Phys. Rev. B* **5**, 4966 (1972).
- <sup>55</sup>P. M. Chaikin, A. F. Garito, and A. J. Heeger, *J. Chem. Phys.* **58**, 2336 (1973).
- <sup>56</sup>P. J. Strebelle and Z. G. Soos, *J. Chem. Phys.* **53**, 4077 (1970).
- <sup>57</sup>J.-J. Chang, S. Jafarey, and D. J. Scalapino (unpublished).
- <sup>58</sup>R. E. Merrifield, *Phys. Rev. Lett.* **34**, 87 (1975).
- <sup>59</sup>J. B. Torrance and B. D. Silverman (unpublished).
- <sup>60</sup>V. E. Klymenko, V. Ya. Krivnov, A. A. Ovchinnikov, I. I. Ukrainsky, and A. F. Shvets, report (unpublished).
- <sup>61</sup>J. S. Miller and A. J. Epstein, *Prog. Inorg. Chem.* **20**, 1 (1976).
- <sup>62</sup>W. D. Grobman, R. A. Pollak, D. E. Eastman, E. T. Maas, Jr., and B. A. Scott, *Phys. Rev. Lett.* **32**, 534 (1974).
- <sup>63</sup>B. H. Schechtman, S. F. Lin, and W. E. Spicer, *Phys. Rev. Lett.* **34**, 667 (1975).
- <sup>64</sup>C. R. Ginnard, R. S. Swingle, II, and B. M. Monroe, *J. Electron Spectrosc. Relat. Phenom.* **6**, 77 (1975).
- <sup>65</sup>P. Nielsen, D. J. Sandman, and A. J. Epstein, *Bull. Am. Phys. Soc.* **20**, 465 (1975); *Solid State Commun.* **17**, 1067 (1975).
- <sup>66</sup>F. Denoyer, F. Comés, A. F. Garito, and A. J. Heeger, *Phys. Rev. Lett.* **35**, 445 (1975).
- <sup>67</sup>I. I. Ukrainsky, report, Kiev, 1974 (unpublished) (as quoted in Ref. 52).
- <sup>68</sup>R. M. Metzger and A. N. Bloch (unpublished).